Volume 58, Issue 2, 2021 ***e-ISSN (online):*** *2300-8830*

DOI: *10.5604/01.3001.0014.8797*

ENERGY MANAGEMENT SYSTEM OF THE HYBRID ULTRACAPACITOR-BATTERY ELECTRIC DRIVE VEHICLES

Ireneusz PIELECHA

Poznan University of Technology, Faculty of Civil and Transport Engineering, Poznan, Poland

Abstract:

The search for new, alternative propulsion and energy sources in transport is one of the economic and technological priorities of the current decade. The modern development of hybrid drives and electric means of transport makes it possible to at least partially diversify conventional drive systems. The study discusses the use of a battery and ultracapacitor in electric vehicles. Simulation analyzes of energy flow were performed using the solutions of electric drive systems and various energy storage control algorithms. The research was carried out in relation to the use of braking energy, its conversion into electricity and its storage in a battery or ultracapacitor. The operating conditions of the battery and the ultracapacitor were assessed in terms of specific energy consumption while driving. The article proposed the use of a drive system connected in series, the last link of which was an ultracapacitor. Such a solution significantly reduced the use of the battery as well as its regular charging-discharging. At the same time, it required the use of a high-capacity ultracapacitor, which contributed to increasing its charging time. The analyzes were carried out using standardized research tests as well as tests in real traffic conditions. The research was carried out with the use of the AVL Cruise software for the analysis of energy flow in vehicles; a middle class passenger vehicle was selected for the tests, equipped with an electrochemical battery and – in the next stage of the research – an ultracapacitor. Three research models were used: I) typical electric drive system; II) a system with the use of ultracapacitors ran by a simple control algorithm; III) a system with the use of ultracapacitors with an advanced control algorithm (the algorithm took into account the change of driving conditions to the ultracapacitor charging conditions). The advantages of using ultracapacitors in the electric drive of a vehicle were demonstrated, especially for results obtained in real traffic conditions. Analyzing the simulation tests results allowed to determine the most advantageous options of utilizing these systems, in particular in the aspect of increased possibilities of algorithms controlling the flow of electricity in the drive system.

Keywords: *electric vehicle, battery, ultracapacitor, energy flow modeling*

To cite this article:

Pielecha, I., 2021. Energy management system of the hybrid ultracapacitor-battery electric drive vehicles. Archives of Transport, 58(2), 47-62. DOI: https://doi.org/10.5604/01.3001.0014.8797

Contact:
ireneusz.pielecha@put.poznan.pl [https://orcid.org/0000-0001-7340-635X]

1. Introduction

1.1. Vehicle electric drives

The diversification of conventional means of transport mainly concerns the use of hybrid (diesel-electric) and electric drives. Ultimately, both of these groups should be complemented by a fuel cell drive (FCHEV). In 2018, sales of alternative drives in Europe amounted to 59% – HEV, 21% – BEV and 19% PHEV (plug-in). In 2019, the share of vehicles with electric drives increased significantly and the market structure became: 56% – HEV, 28% – BEV and 16% PHEV (Jato Dynamics Limited, 2020).

According to the Polish Alternative Fuels Association (2020), at the end of June 2020, 12,271 electric passenger cars were registered in Poland, 56% of which were BEVs – 6,837 units, the rest were PHEV – 5,434 units. Number of electric vehicles classed as trucks and vans in the analyzed period included 606 units. The number of electric mopeds and motorcycles at the end of June 2020 reached the number of 7342 units. The number of electric buses in Poland in the same period was 296 units. Compared to the corresponding period of 2019, this means a number increase by 116%.

1.2. Use of batteries

The modern development of electric vehicles is determined by the development of energy storage devices. The main focus is on electrochemical batteries (Sun, et al., 2019, Pielecha & Pielecha, 2020). Initially, lead acid batteries had a low energy density, between 20 and 40 Wh/kg (Miller, 2009). To obtain a range of 200 km, it was necessary to equip the vehicle with batteries weighing about 500 kg (Offer, et al., 2010). The energy density of Ni-MH batteries is much higher and amounts to 60-80 Wk/kg (Miller, et al., 2009), which enables their use in electric vehicles. However, their most common use is currently in vehicles with hybrid drive systems (Pielecha, et al., 2018). Despite that they are being widely replaced by Li-Ion batteries. This type of energy storage has a high energy density, because lithium possesses both the highest electrochemical potential and a low equivalent mass (Deberitz, 2006). The energy density of such batteries is 150-210 Wh/kg (Xia, et al., 2015, Sharma, et al., 2020). However, the significant disadvantages of lithium-ion batteries are their very high production cost and overcharging, or heating above 100°C, which causes the decomposition of the positive electrode and the electrolyte while releasing dangerous gases (Xia, et al., 2015).

The $Na/NiCl_2$ battery technology (Sodium Nickel Chloride, Zebra) has many advantages (low cost, high number of effective charge cycles), but also the disadvantage of low power (about 150 W/kg). Despite the similar energy density to Li-Ion batteries (of about 120 Wh/kg), they are not widely used in BEVs (Tie & Tan, 2013).

Lithium-based battery is one of the promising battery technologies with high energy density, high power density and one that can quickly receive a large amount of energy. Lithium-based batteries dominate the most recent group of EVs. A few established battery types fall under the category of a lithium-based battery, such as lithium-ion (Li-Ion), lithium-ion polymer (LiPo) and lithium-iron phosphate ($LiFePO_4$) (Yong, et al. 2015, Vukajlovic, et al., 2020).

Due to the need to recharge the batteries of electric vehicles, "travel safety" is significantly limited. In addition, differentiated charging systems and power connections and their charging power do not increase the advantages of electromobility (Das, et al., 2020).

Often, the operating modes of electric vehicles are characterized by their maximum speeds (Armenta et al., 2015):

– eco mode: the vehicle can reach a maximum speed of 120 km/h, therefore increasing the vehicle travel range is the main determinant of the control algorithm quality for such a system. Discharge current values are less than standard.
– sport mode: can reach a maximum speed of 160 km/h, priority is given to vehicle acceleration over range.

Diagnostics of vehicles equipped with internal combustion engines uses both direct and indirect methods. Most often, however, indirect methods are used (such as exhaust emissions analysis, OBD diagnostics of the engine and other systems). Direct methods (indicators, optical) often require direct access to the engine cylinder.

Diagnostics of electric vehicles, on the other hand, is currently carried out using mainly direct methods. This enables accurate measurement of voltage-current values, taking into account the efficiency of the systems. However, this necessitates partial interfer-

ence into the vehicle's electrical systems (Apostolaki-Iosifidou, et al., 2017, Polak, 2020, Valdez-Resendiz, et al., 2020).

1.3. Use of ultracapacitors

Electric vehicles are often equipped with additional energy storage systems such as ultracapacitors. This is a system with high power density and low energy density. This makes quick charging and discharging of such a system possible. There are many solutions for using ultracapacitors in combination with batteries (Armenta, et al., 2015) as well as batteries and fuel cells (Bubna, et al., 2012).

Xiong, et al. (2018) in his work presents several solutions for the parallel connection of batteries and ultracapacitors. In the passive version, the system does not include DC/DC converters that match the voltage levels of both systems. The semi-active version (Xiong, et al. 2018, Asensio, et al., 2020) includes one of two connection variants: both a series connection of one of the energy sources with a DC/DC converter. The fully active model includes two DC/DC converters in series with the two energy sources, which are later connected in parallel (Kasimalla, et al., 2018).

Extensive use of ultracapacitors can also be observed in fuel cell systems. In such systems, the fuel cell, battery, and ultracapacitor are often connected in parallel, both in motor vehicles (Fu, et al., 2020) and heavy-duty vehicles (Bubna, et al., 2012). Bubna et al. (2012) showed that increasing the number of ultracapacitors in a system reduces the amount of heat generated from such a system with regard to electrochemical batteries (even by as much as 50%).

2. Research aim

Electric vehicles are equipped with various types of batteries, currently the most common of these are Li-Ion batteries. However, the battery solutions, due to the specific use of materials, are also quite diverse. The aim of the article is therefore to present an alternative method that allows the use of ultracapacitors in the electric drive of the vehicle. Although such systems are already used, the paper proposes a series connection with the battery in such a way as to use a high-voltage battery to a limited extent. On the one hand, it increases the complexity of the system, but on the other hand, it allows to reduce the number of charging and discharging cycles of the battery, thus extending its lifespan. This increases drive system durability and allows for quick storage of the electric charge necessary for further vehicle drive. Other advantages of using an ultracapacitor, in the form of increased voltage and current values, make them now widely used also in hybrid drive systems.

3. Method

3.1. Testing conditions

The research was conducted using three chosen research models:

Model I – using only the battery (BAT) alone. Its control conditions include typical discharge and regenerative charging in accordance with the strategies outlined below.

Model II – uses an ultracapacitor (UCAP) connected in series with the BAT. The discharge conditions typical for full hybrids with plug-in systems were used in this model, i.e. charge depleting and charge sustaining (Nemry, et al., 2009, Takaoka, et al., 2010). This means that in the initial driving conditions, the UCAP was discharged to the point where recharging would begin. This state was maintained until the end of the test. Such control was aimed at limiting the discharge of the battery towards both the vehicle drive as well as to the UCAP.

Model III – using the same setup as previously (Model II) with the addition of a more complex energy flow control system from the UCAP. The structure of the system does not change, only the algorithm controlling the UCAP charge level is adjusted. In this system, the UCAP charging conditions were additionally made dependent on the vehicle speed. It included three conditions (described later). Additionally, UCAP charging off switch was connected to the vehicle braking (regardless of its state of charge).

3.2. Software and vehicle model

The analysis of the possible applications of UCAP in a 1315 kg electric drive was carried out using the AVL Cruise software (Fig. 1). The system uses – slightly different from those presented in the first part of the article – an in series UCAP connection with a BAT. This solution forces the use of UCAP in all operating conditions of the drive system, thus limiting the use of the BAT (all using an appropriate control algorithm). This means that the capacitor used should have a much greater electrical capacity than what is necessary to be able to store all the energy obtained during the longest vehicle braking

during the most dynamic drive test. The main specifications of the analyzed vehicle were provided in Table 1.

Table 1. Test vehicle specifications

Parameter	Unit	Value
Wheelbase	m	2.467
Frontal surface	m^2	1.97
Mass	kg	1315
Gross weight	kg	1580
Transmission ratio	–	6.058
Static rolling radius (wheel)	m	0.287

The vehicle model shown in Fig. 1 contains a visualization of the mechanical connections of the drive system (in blue). Electrical connections between elements were shown in red. The UCAP and the DC/DC converter systems have been implemented only in models II and III. In addition, there are elements in the system that do not have connections in Fig. 1 (such as the Cockpit, Online monitor). These elements are integrated with other circuits by means of logical connections. The same connections apply to the group of elements marked in green (Constants, eBrake, eDrive and Function DC_DC). The latter are described in detail later in the article.

Below is an analysis of the module content, which is of particular importance for further research.

1) Constants. This module contains constant values. There are, among others values determining the maximum pressure in the braking system (5 MPa), value of the main gear ratio (i_{FD} = 6.058) as well as braking coefficients (front – B_F; rear – B_R) which are the components of the braking torque. This torque value was calculated using the product:

$$M_B = 2p_B \cdot A_B \cdot \eta_B \cdot \mu_B \cdot r_B \cdot c_B \quad (1)$$

and the braking coefficients were determined using the relation:

$$B = \frac{M_B}{p_B} \quad (2)$$

For the front and rear axle respectively:

$$B_F = 2 \cdot A_{BF} \cdot \eta_{BF} \cdot \mu_{BF} \cdot r_{BF} \cdot c_{BF} \quad (3)$$
$$B_R = 2 \cdot A_{BR} \cdot \eta_{BR} \cdot \mu_{BR} \cdot r_{BR} \cdot c_{BR} \quad (4)$$

where: p_B – current pressure value in the brake system, A_B – the brake cylinder area; the area of the hydraulic cylinder (front – A_B = 0.0018 m^2; rear – A_B = 0.0015 m^2, h_B – the efficiency considers the effects of the conversion of hydraulic into mechanical force in part of the brake (h_B = 0.99), m_B – the friction coefficient is determined between the brake drum, the friction disc and the brake shoes respectively (m_B = 0.25), r_B – the radius where the braking force is applied (front – r_B = 0.13 m; rear – r_B = 0.11 m), c_B – the specific brake factor is a factor that depends on the design of the brake (disc brakes c_B = 1; drum brakes c_B > 1).

An overview of the values indicated above was listed in Table 2.

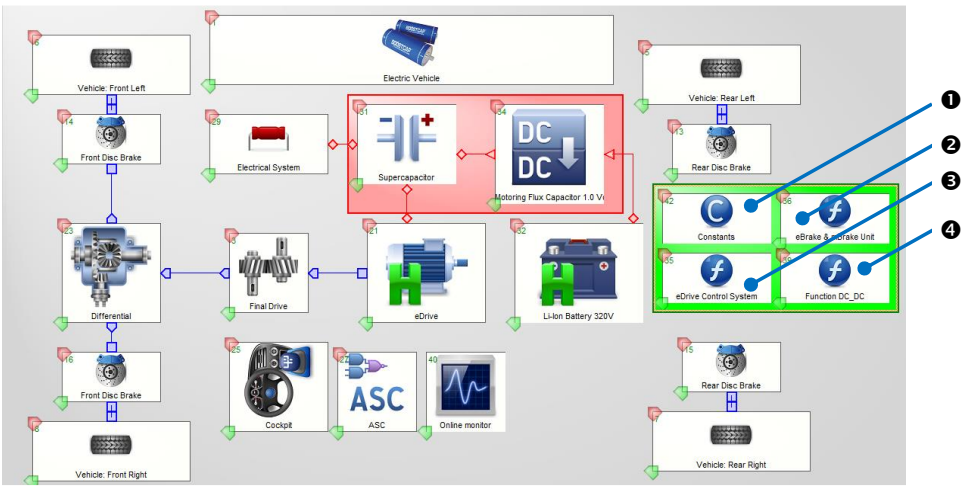

Fig. 1. Model of an electric vehicle drive system equipped with ultracapacitors

Table 2. Example values of parameters and constants

Parameter	Value	Unit	Determined using
Brake factor front (B_F)	0.00011583	–	Equation (7)
Brake factor rear (B_R)	0.000081675	–	Equation (8)
Max brake pressure (BP_{max})	50	bar	Assumed in AVL Cruise (2020)
Brake factor C_{BF}	1	–	Selected for simplicity

2) eBrake & mBrake Unit. Converting brake torque into pressure for all brakes (Front & Rear). When calculating the braking torque of the electric motor (M_{EM}), the ratio in the main gear should be taken into account ($i_{FD} = 6.21$). Based on the equation (4), substituting the braking torque with the electric motor torque and taking into account the i_{FD} ratio and the current pressure in the braking system, the following relation was obtained:

$$P_B = \frac{M_{EM} \cdot i_{FD} \cdot i_G}{2 p_B \cdot A_B \cdot \eta_B \cdot \mu_B \cdot r_B \cdot c_B} \tag{5}$$

and assuming the coefficients B_F (equation (3)) and B_R (equation (4)) as the sum of the braking coefficients:

$$p_B = \frac{M_{EM} \cdot i_{FD}}{B_F + B_R} \tag{6}$$

the pressure values in the braking system were obtained, which can be converted into electric braking (energy recuperation). If electric motor braking is used, then p_B (i.e. eBrake) takes negative values (negative torque value). In this case, electric braking would be used first, and if the braking performance requires additional pressures – then braking with the use of the hydraulic system would be activated. If $M_{EM} > 0$, this motor transfers a positive torque value to the wheels of the vehicle (propelling the vehicle).

3) eDrive Control System. The algorithm determines the conditions for the transition from eDrive to eBrake. The necessary condition for the use of regenerative braking is the simultaneous fulfillment of two relationships (increase in pressure in the brake system and vehicle speed above a certain value):

$$\begin{cases} \text{Brake Pressure} > 0 \\ \text{Vehicle velocity} > 0.1 \text{ km/h} \end{cases} \tag{7}$$

If those conditions are met braking begins, where the control signal (activating the hydraulic brake) is defined as the ratio of the current brake pressure – BR to the maximum system pressure BR_{max} taking into account the possible brake boost C_{BF}:

$$y = \frac{BR}{BR_{max}} \cdot C_{BF} \tag{8}$$

Taking into account the above provision, the value of the braking force $C_{BF} = 1$ was implemented in modules II and III. Decreasing the value of $C_{BF} < 1$ reduces the contribution of regenerative braking, which at the same time reduces the final SOC value of the battery at the end of the test drive.

4) Function DC_DC – is the voltage converter system. The use of an UCAP and a battery requires matching the voltage and current levels of these two systems. The implemented system makes it possible to recharge the battery only in model I. In other cases, the electric capacity of the UCAP is sufficient to accumulate the charge without recharging the battery at all.
The Boost Converter can be described with an equation (without taking into account power losses):

$$P_{DC,LV} = P_{DC,HV} \tag{9}$$

where DC means direct current, and symbols LV and HV mean the lower and higher voltage respectively.
By expanding the above equation we obtain:

$$U_{DC,LV} \cdot I_{DC,LV} = U_{DC,HV} \cdot I_{DC,LV} \tag{10}$$

If the power losses are taken into consideration the basic equation would be defined as:

$$P_{DC,LV} = P_{DC,HV} + P_{DC,loss} \tag{11}$$

where $P_{DC,loss}$ means the loss of power on the DC/DC converter.
The actual power loss in the DC/DC converter is the total loss of power on the electronic elements such as inductance, internal resistance, diodes, etc.
The last element of the electric drive control system (DC/DC) was also used to determine the energy flow control strategy by switching it on or off. Three control strategies (three models) of the system have been implemented and tested in the simulation program:

I. enables the BAT to be used to power the electric motor and energy recovery (with no other energy storage system); the operation of the regenerative braking system is the same in each case;
II. the use of an UCAP prevents the recharging of the BAT; the control strategy only includes meeting the boundary conditions for charging and discharging the UCAP; these limits were established with the values: start – SOC_U_s = 50% and end – SOC_U_e = 55%;
III. a strategy based on a set of factors:
   a. enabling the UCAP charging:
      1) SOC_U < 45%;
      2) SOC_U < 50% and V_{veh} > 15 km/h;
      3) SOC_U < 55% and V_{veh} > 90 km/h (protection against too rapid energy discharge);
   b. disabling the UCAP charging:
      1) braking (independent of SOC_U);
      2) SOC_U >= 60%.

3.3. Ultracapacitor selection

The selection of UCAP when chosen for use in traditional (parallel) systems consists of calculating the dynamic conditions (the kinetic energy of the vehicle E_{kin}) and comparing them with the conditions of collecting electric energy E_{el}. If the efficiency of energy transfer is omitted, the equation has the form:

$$E_{kin} = E_{el} \tag{12}$$

by expanding, it can be expressed as:

$$\frac{1}{2}m(v_2^2 - v_1^2) = \frac{1}{2}C \cdot (U_e^2 - U_s^2) \tag{13}$$

where: m – vehicle mass (m = 1315 kg), v – velocity, maximum and final when braking respectively (v_2 = 130 km/h; v_1 = 0 km/h; the maximum speed during braking to a standstill occurs in the RDC test), C – the calculated energy capacity of the UCAP, U – voltage, respectively: at the end and the beginning of the UCAP charging.
Determining the electric capacity of a capacitor provides:

$$C = \frac{m(v_2^2 - v_1^2)}{U_e^2 - U_s^2} \tag{14}$$

In relation to the proposed concept, based on the equation (Rambaldi, et al., 2011), the resulting power on the vehicle wheels P_w was determined:

$$P_w = V \cdot (m \cdot g \cdot \cos\alpha) \cdot (f_0 + kV^2) + \frac{1}{2}\rho V^2 A C_x + V m_g \sin\alpha + V m_e a \tag{15}$$

where: V – vehicle speed, m – vehicle mass, g – gravitational acceleration, a – road slope, f_0 – static resistance coefficient of tires, k – dynamic resistance coefficient of tires, r – specific weight of dry air, A – frontal surface area of the vehicle, C_x – drag coefficient.
The ultracapacitor was selected based on the results obtained by analyzing the maximum values of this power in each of the research tests. Taking into account its operating conditions (wide values of voltage and current changes), the system used a DC/DC voltage converter with a power of 40 kW. Such high power was necessary to limit the unfavorable changes in the electric capacity of the UCAP during its discharge. This limited its maximum discharge, preventing interruptions in the flow of energy to the electric motor. Additionally, the energy supplied from the BAT ensured that the UCAP system was discharged to a minimum value.
The drive train used an electric motor with a power of 75 kW and a maximum torque of 240 Nm. A battery with an electric capacity of 50 Ah and a nominal voltage of 320 V was used (nominal power is 16 kW). The characteristics of electrical systems (engine, BAT, UCAP and DC/DC converter were included in Table 3.

4. Drive system evaluation

4.1. Analysis of driving conditions

The energy flow studies were carried out on three test routes: New European Driving Cycle – NEDC, Worldwide Harmonized Light-Duty Vehicle Test Procedure – WTLP, class 3b (for vehicle with V_{max} > 130 km/h) and in Real Driving Cycle (RDC) based on Poznan measuring section (city, rural and motorway) – Table 4. Using only the driving profile and not the exhaust emissions for simulation tests, the RDC designation was used instead of RDE (Real Driving Emissions).

Table 3. Characteristics of the electrical systems of the analyzed model

Parameter	**Unit**	**Value**
Electric motor		
Type of machine	–	Asynchronous motors
Max torque	Nm	240 (0–3000 rpm)
Max power	kW	75 (3000–7000 rpm)
Max efficiency	% (Nm/rpm)	93.0 (180/4000) 90.5 (225/3000)
Nominal voltage	V	320
Inertia moment	kg m^2	1.0E–4
Maximum speed	rpm	10,000
Battery		
Maximum charge	Ah	50
Nominal voltage	V	320
Maximum voltage	V	420
Minimum voltage	V	220
Number of cells (per cell/rows)	–	1/5
Internal charge/discharge resistance	W	0.8/0.6
Initial charge	%	95
Ultracapacitor		
Capacitance	F	70
Nominal voltage	V	336
Minimum voltage	V	300
Maximum voltage	V	500
Maximum current	A	600
Initial charge	%	60
Line resistance	W	1.0E–12
DC/DC converter		
Max converter power	kW	40
Higher voltage Max/min/nominal voltage	V	420/220/320
Lower voltage Max/min/nominal voltage	V	600/200/350
Efficiency	%	95 (constant)

Table 4. Comparison of driving tests used in simulations

Parameter	**NEDC Test**	**WLTP Test**	**RDC Test**
Test cycle	Single test cycle	Dynamic cycle	Real driving
Cycle time	20 min	30 min	96 min
Cycle distance	11 km	23.25 km	75.328 km
Average speed	34 km/h	46.5 km/h	46.97 km/h
Maximum speed	120 km/h	131 km/h	133 km/h
Driving phases	2 phases: 66% urban, 34% non-urban driving	4 dynamic phases: 52% urban, 46% non-urban	3 dynamic phases and stop: 34% urban, 26% rural, 39% motorway, 26% stand-still in urban route

The analysis of the test routes (Fig. 2) showed a large variation in driving conditions. The shares of urban sections were different, which means that the drive system operation could also be expected to vary. In the case of slight changes in acceleration and deceleration of the vehicle, the algorithms used might not result in significant differences in the final estimates of the tested models. Due to the different traffic conditions, the vehicle acceleration values are the highest in the RDC test. One should emphasize that these accelerations were greater in the NEDC test than in the WLTP test (Fig. 3a).

Research on the electric motor operation showed the most extensive use of the engine operating range in the RDC test (Fig. 3b). The WLTP test had a lower torque requirement – around 30 Nm less than in the NEDC test. The use of the braking torque in these

two tests was also different. Higher values of the braking torque were recorded in the WLTP test than in the NEDC test. This means that the WLTP test conditions should be conducive to regenerative braking (torque values approximately 50% higher than in the NEDC test). The highest values of the braking torque were observed in the RDC test and they were about 5 times greater than in the NEDC test.

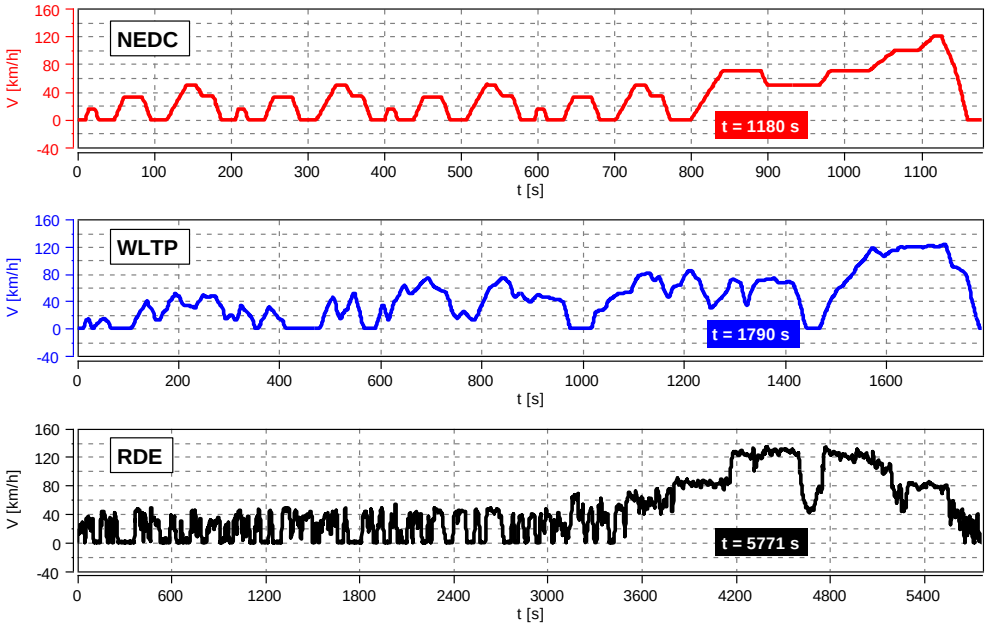

Fig. 2. Driving conditions for the test drives – routes used

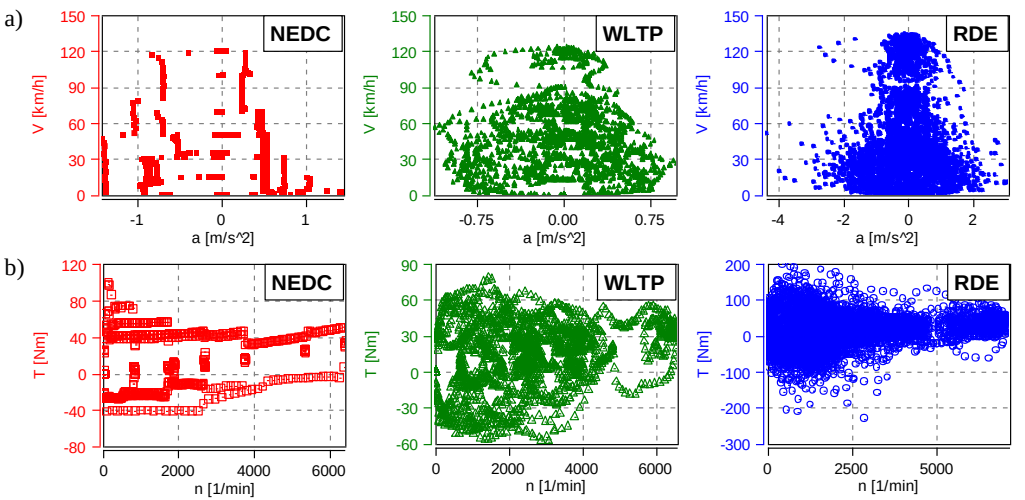

Fig. 3. Assessment of drive system operation conditions in research tests of: a) vehicle, b) electric motor

4.2. Battery and ultracapacitor discharge analysis

The implemented models and algorithms make the analyzed systems work as follows:

– model I – energy recovery for the battery (without the UCAP),
– models II and III – energy recovery only to the UCAP.

For this reason, the electric capacity of the battery largely determines the vehicle range. Despite the energy recovery system operating as intended, a continuous decrease in the SOC of the battery could be observed, regardless of the control model used (Fig. 4). This means that even in the case of the first model, without the UCAP, the energy recovery was not significant in terms of the electric capacity of the entire system. The greatest differences between the tested control models in terms of SOC changes were noted in the case of the NEDC test. Models using UCAP kept the battery SOC high for much longer. In the case of the longer drive tests (WLTP and RDC), the differences were comparably small. Each of the analyzed cases indicated that the greatest drops in SOC were related to increased driving speeds. This means high energy consumption and limited chance of energy recovery.

Assuming that the battery parameters are in accordance with Table 3, the resistance dependence of the battery load was obtained in Fig. 5a. The values of the discharge resistance R_{dch} reach 0.123 W, and when charging it, R_{chg} = 0.152 W. Taking into account the equation determining the battery efficiency:

$$\eta_{BAT} = 1 - \frac{I^2 \cdot R_{chg/dch}}{U \cdot I} \text{ [-]} \tag{16}$$

the characteristic of its efficiency was obtained (Fig. 5b).

The use of UCAP makes it possible to recover braking energy as well as to recharge them using the battery. The system's operating strategy depends on its charging from two independent sources. The UCAP charge was assumed to be 60% at the start of the tests. This value was adopted due to the possible necessity to accelerate after starting the drive and the simultaneous lack of energy flow from the BAT. Only strategies 2 and 3 were analyzed (the first model does not include UCAP).

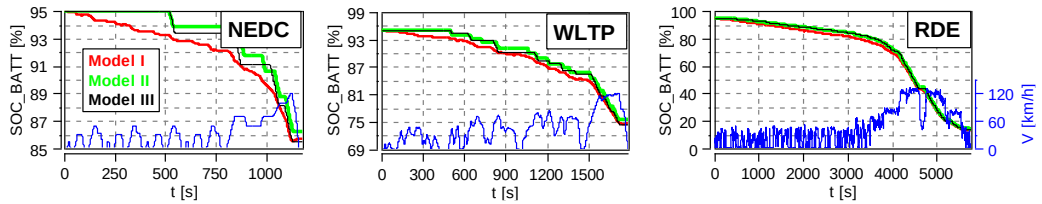

Fig. 4. Analysis of battery SOC changes during three driving test routes for different vehicle drive system models

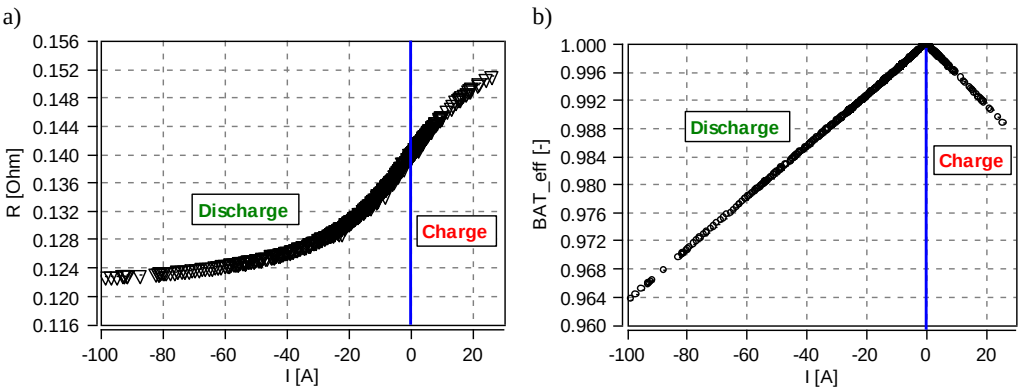

Fig. 5. Battery characteristics: a) instantaneous internal resistance of the battery, b) change of the efficiency during battery operation

Model III enabled better adjustment of the actual UCAP capacity to the driving conditions at a given time. In each of the three routes (Fig. 6), an increase in the UCAP SOC when driving at higher speeds was visible. This directly relates to increasing the safety buffer and "preparing" the system for increased energy consumption. Regarding the NEDC test, the differences between the two models (at increased driving speed) averaged around 3%. The maximum difference was 10% (at t = 860 s). Completion of the NEDC test was associated with an approximately 5% higher SOC for model III.

The analysis of the WLTP test showed the different UCAP operating conditions. This was especially true at high travel speeds (t > 1500 s). Then the differences in the SOC of both control models amounted to about 5%. The final value of the WLTP test indicated a higher SOC in model III by about 5% (which was similar to the value obtained in the NEDC test).

The actual RDC driving conditions indicated that even lower driving speeds (500 s < t < 4000 s) caused discrepancies in the UCAP operating conditions. As it was with the extra-urban and motorway speeds in previous tests, an increase in the UCAP SOC range was also observed in this case. The highest vehicle travel speed conditions caused the SOC differences to be about 5% in the analyzed models. Such differences resulted from the higher allowable electric capacity of the UCAP system used in model III (details of the control system used were presented in section 3.2).

The conditions of current flow and voltage changes in the UCAP were quite varied (Fig. 7). They result from the specificity of such a system. In the analyzed system (according to Table 3), the permissible voltage changes resulted in much higher current values in model II compared to model III. The discharge conditions of the UCAP were similar (negative current values and powers), while when charging those values were much higher (in model II). This was mainly due to the continuous topping-up of the UCAP charge.

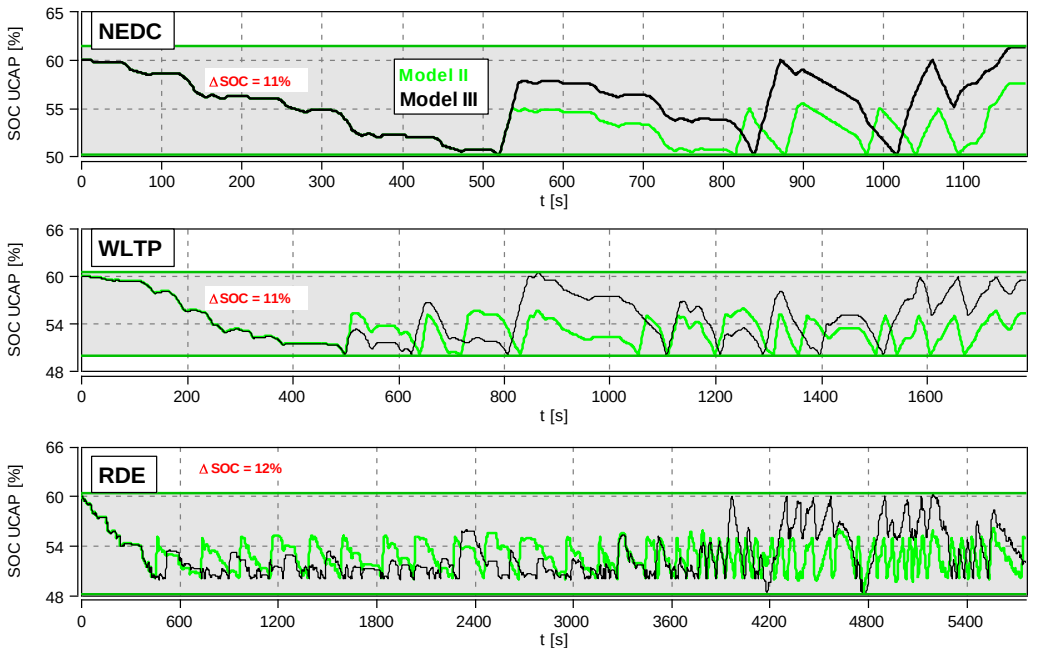

Fig. 6. Ultracapacitor discharge analysis in three driving routes for two drive models (model II and model III; model I – only had a battery)

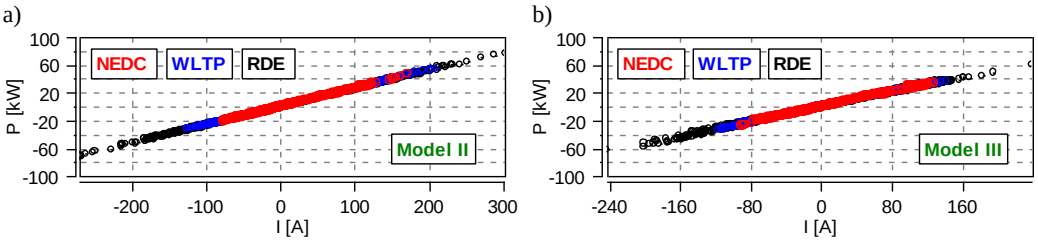

Fig. 7. Assessment of ultracapacitor: a) charging and b) discharge conditions during three test routes

The presented charging and discharging conditions of the systems made it possible to determine the total energy supplied to the UCAP (from the braking energy recovered as well as from the electrochemical battery). The analysis of the data in Fig. 8 showed that using a drive system design with only a battery system in the electric vehicle made it possible to recover energy at a rate from about 0.23 Ah (NEDC test) through 0.433 (WLTP test) up to about 1.78 Ah (RDC test). The amount of energy recovered from braking depends in this case on the traffic conditions. When the RDC test was performed driving dynamically made it possible to accumulate about 8 times more energy than in the NEDC test. The analysis of energy consumption and gain allowed to determine the share of the recovered electric capacity of the battery (proportional to the SOC):

– in the NEDC test – 4.7% (4.88 Ah – consumed/0.23 Ah – gained),
– in the WLTP test – 4.1% (10.6/0.43),
– in the RDC test – 4.2% (42.7/1.78).

The use of UCAP resulted in significantly higher values of energy stored. This was mainly due to the way the system worked – the charging of the capacitor was done by recharging from the battery (to a large extent) as well as from regenerative braking.

4.3. Assessment of energy consumption in drive tests

The use of different algorithms controlling the drive system led to a different operation of the battery and the UCAP. This was then reflected in energy consumption (Fig. 9). The use of UCAP caused the differences in the specific energy consumption during the NEDC test reach approx. 15% (t = 700 s). The final differences were around 9%. These changes were the result of high travel speed values which – regardless of the control method – require increased energy expenditure. The resulting differences between the UCAP models were minimal (less than 1%). Analysis of the WLTP test shows smaller SEC differences. After t = 1000 s, the difference was about 11%, while during the entire test it was reduced to 7%. The dynamic RDC test showed that there were even greater differences between urban and suburban driving. At t = 1800 s, the differences in SEC reached about 20%. Longer time spent driving in motorway conditions required greater energy expenditure, which explains why the final observed differences were about 6%.

It should be noted that regardless of the type of test route used for the drive, the differences in the operation of the control algorithms were the same.

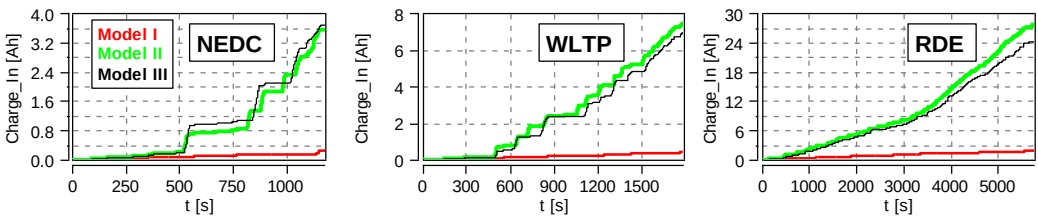

Fig. 8. Total energy delivered to the ultracapacitor (or to the battery for model I) during the drive tests

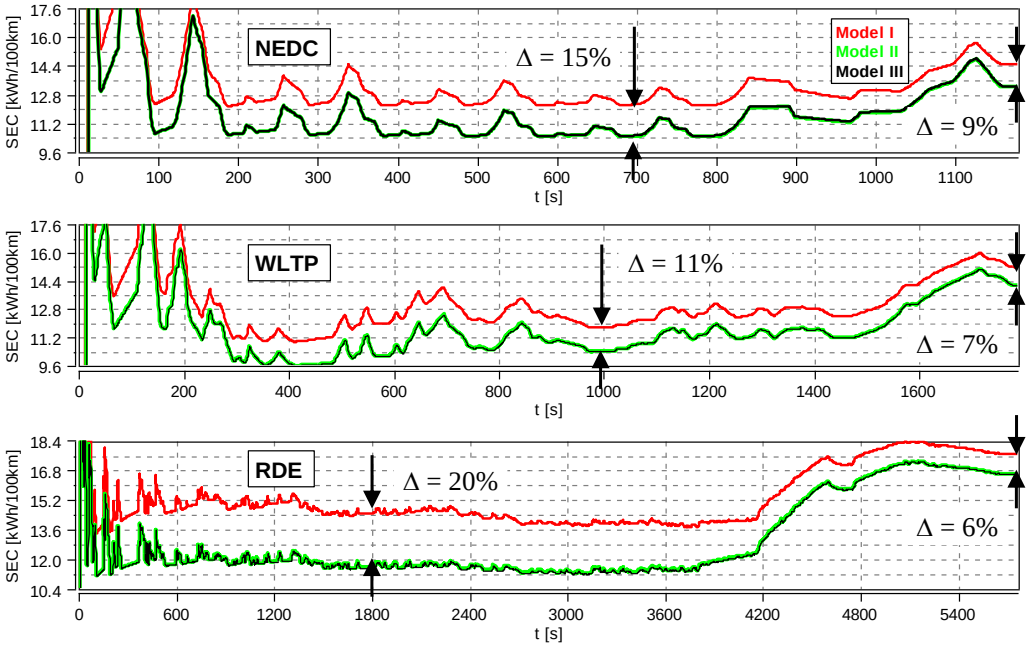

Fig. 9. Analysis of the vehicle specific energy consumption during the tests of the three drive system models

It follows that more advanced control algorithms reduce the energy consumption of an electric vehicle, even as the number of electrical systems increases. Increasing the efficiency of these additional systems (DC/DC converter and UCAP) would slightly change the operating conditions. This is due to the high efficiency values of such systems (about 95%).

5. Energy assessment of the drive systems

The use of various control algorithms in electric vehicle drives makes it possible to shape and control the flow of electric energy. This control increases thanks to the use of ultracapacitors by enabling new options for energy management. The drive system used in the research was a series connection of a battery and an UCAP. The biggest changes in the battery SOC were recorded in the RDC test; and those changes were the greatest in the system model without the UCAP (as it was in the case of the NEDC test). Although the model I does not include the UCAP, the change (decrease) of the battery SOC in the other two driving tests was not the greatest for this model's system configuration (Fig. 10). In the WLTP test, the greatest change in the SOC of the battery was observed when using the model III. Drive systems that incorporated a UCAP, regardless of the control model, showed different variations of the battery SOC.

Changes in the UCAP SOC indicated a large variation in the final charge level (Fig. 11). Model III showed an increase in SOC (in the NEDC and WLTP tests). In the last drive test a decrease in SOC was observed for this system. The smallest changes in SOC were found in the NEDC test, the largest – in the RDC test. For model II, the increase in the UCAP SOC was found to correlate together with the dynamics of tests (NEDC → WLTP → RDC). In the case of model III, there is no such unequivocal relationship: first, an increase was observed, and then increasingly greater decreases in SOC. Despite the fact that the instantaneous drops reached the minimum values, the characteristics of the test drives (a lot of braking at the end of each test) resulted in a significant energy recovery to the UCAP. As a result the final SOC values do not reach the minimum values.

Due to large changes in speed and acceleration in the RDC test, the instantaneous UCAP SOC changes are much smaller than the adopted nominal values (as-

suming an increase in UCAP charging from the battery). This means that the adopted models do not ensure that the UCAP SOC falls below the minimum values. In this case it would be necessary to estimate SOC changes taking into account travel routes. Such conditions are possible to implement for a route recorded using navigation, but they seem unrealistic to use for an unknown route.

By considering the overall operating conditions of the battery and the UCAP, it can be stated that in the NEDC test, due to its steady driving conditions, the change in BAT SOC was relatively small (Fig. 12). It increased along with the dynamics of the driving test (WLTP). The greatest SOC changes were achieved in real driving conditions (RDC test). It is difficult to predict energy consumption from changes in SOC, but the magnitude of changes in BAT SOC can be used as an indicator of the amount of energy consumed. The final UCAP SOC values show a partially similar trend as the changes in the battery SOC. However, it should be noted that the starting UCAP SOC value was 60%.

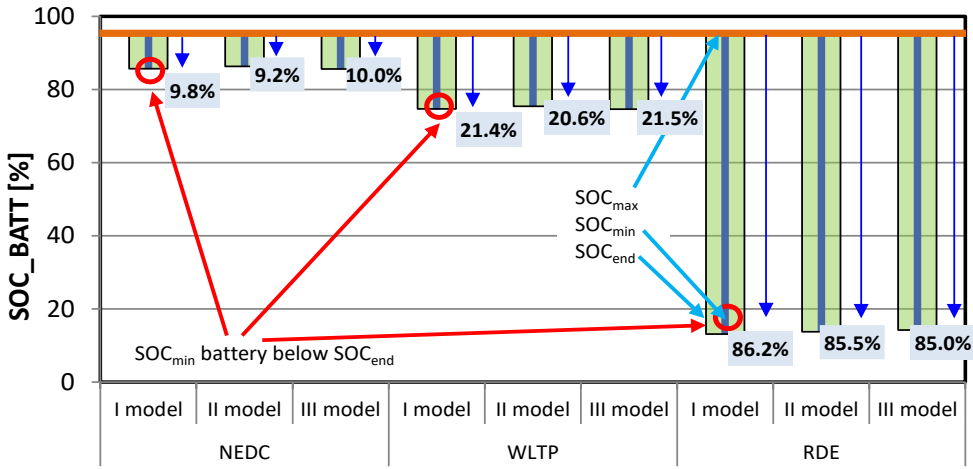

Fig. 10. Assessment of battery operating conditions in driving tests for the three models of vehicle drive system

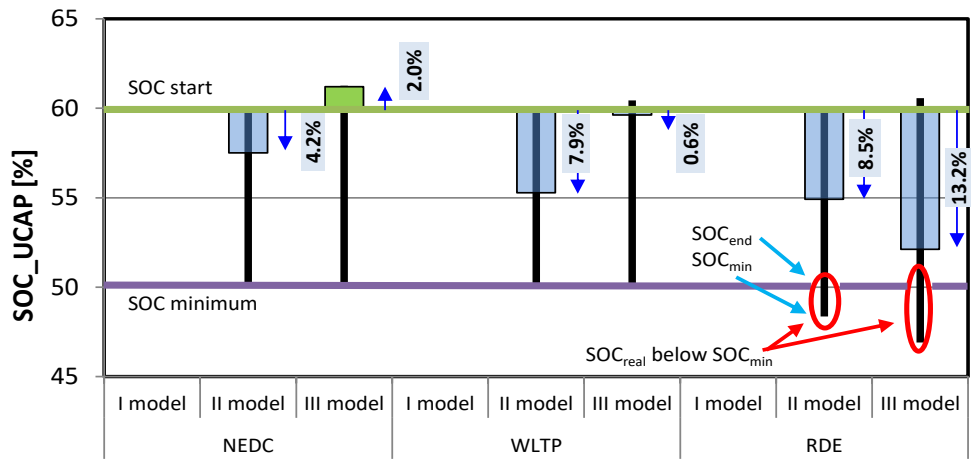

Fig. 11. Assessment of ultracapacitor operating conditions during driving tests for the three vehicle drive system models

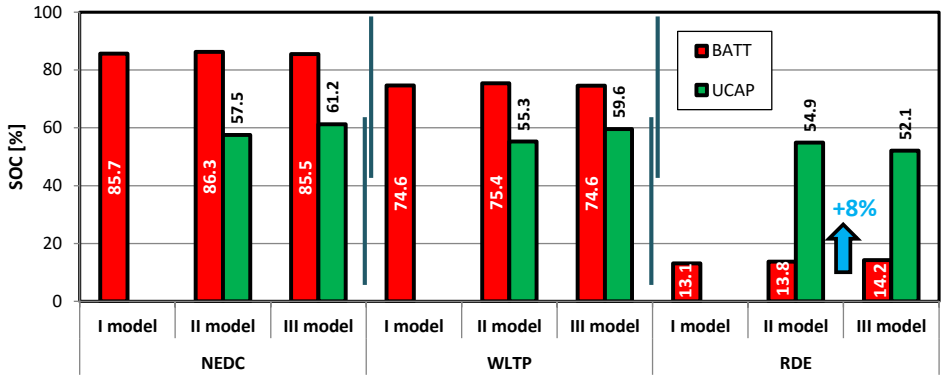

Fig. 12. Summary of battery and ultracapacitor operating conditions during road tests for the three vehicle drive system models

If in the analyzed models II and III battery charging was permitted to occur (and not only charging of the UCAP), then predicting energy consumption could be even more difficult.

The specific energy consumption assessment can only be carried out on the basis of its recorded flow in the system (Fig. 13). Changes in BAT and UCAP SOC alone are insufficient to determine the above figures. The dynamics of the driving tests correspond (in most cases) with the energy consumption. The NEDC test required the least energy input. When using UCAP the obtained SEC was about 10% lower. In the NEDC test, the decrease in SEC with UCAP was smaller – 7%, and in the case of RDC – as low as 6%. Note that using UCAP in the WLTP test resulted in a lower SEC than in the NEDC test (without UCAP). This result indicates the correct use of such a system (a series connection of BAT and UCAP).

6. Conclusions

Pure electric drives (using only a battery) will continue to see limited use. This is because the addition of UCAP in such systems – whether it is connected in parallel or in series – increases the energy management and control options. The presented case of a series drive with different control solutions indicates the possibility of increasing the use of UCAP, and at the same time reducing the energy consumption as determined by the SEC.

Various control models of the BAT+UCAP system indicate the possibility of differentiating the use of the UCAP energy capacity. The more complex control system hardly limits the drop in battery and UCAP SOC. At the same time, such systems require the use of route estimation solutions in order to prevent UCAP SOC from dropping below set critical values.

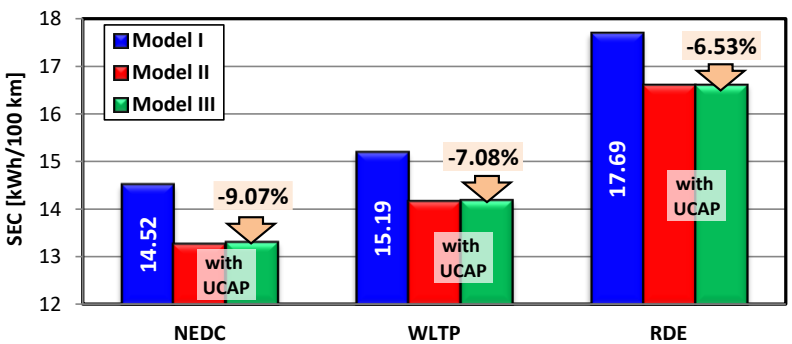

Fig. 13. Specific energy consumption values of vehicles during drive tests for the three vehicle drive system models

The use of series connection of the UCAP and the battery reduces the specific energy consumption:
– in the NEDC test – by about 9%,
– in the WLTP test (with increased driving dynamics) – by about 7%,
– in the real driving conditions – by about 6%.
Using UCAP in an electric vehicle drive increases the vehicle mobility. The use of such a system (with series connection of UCAP and BAT) indicates that with a vehicle range of about 400 km, it is possible to increase its range:
– in the NEDC test – by about 140 km,
– in the WLTP test (with increased driving dynamics) – by about 110 km,
– in the real driving conditions – by about 90 km.
The presented measurable benefits resulting from the addition of UCAP into the vehicle drive systems also require social acceptance of high voltages and currents present in the vehicle during the operation of the electric drive system. In part, these values are acceptable because voltages of 650-800 V are already used in hybrid or electric vehicles.

Acknowledgment
This work has been done under AVL University Partnership Program.

Bibliography
[1] APOSTOLAKI-IOSIFIDOU, E., CODANI, P., & KEMPTON, W., 2017. Measurement of power loss during electric vehicle charging and discharging. *Energy*, 127, 730–742. DOI: https://doi.org/10.1016/j.energy.2017.03.015.
[2] ARMENTA, J., NÚÑEZ, C., VISAIRO, N., & LÁZARO, I., 2015. An advanced energy management system for controlling the ultracapacitor discharge and improving the electric vehicle range. *Journal of Power Sources*, 284, 452–458. DOI: https://doi.org/10.1016/j.jpowsour.2015.03.056
[3] ASENSIO, E.M., MAGALLÁN, G.A., DE ANGELO, C.H., & SERRA, F.M., 2020. Energy management on battery/ultracapacitor hybrid energy storage system based on adjustable bandwidth filter and sliding-mode control. *Journal of Energy Storage*, 30, 101569. DOI: https://doi.org/10.1016/j.est.2020.101569.
[4] AVL Cruise R1, 2020. Advanced Simulation Technologies, Software Documentation. www.avl.com.
[5] BUBNA, P.A., SURESH, G., & PRASAD, A.K., 2012. Integration of batteries with ultracapacitors for a fuel cell hybrid transit bus. *Journal of Power Sources*, 199, 360–366. DOI: doi.org/10.1016/j.jpowsour.2011.09.097.
[6] DAS H.S., RAHMAN M.M., LI S., & TAN C.W., 2020. Electric vehicles standards, charging infrastructure, and impact on grid integration: A technological review. *Renewable and Sustainable Energy Reviews*, 120, 109618. DOI: https://doi.org/10.1016/j.rser.2019.109618.
[7] DEBERITZ, J., 2006. Lithium: production and application of a fascinating and versatile element (2nd ed.), Verlag Moderne Industrie.
[8] FU, Z., ZHU, L., TAO, F., SI, P., & SUN, L., 2020. Optimization based energy management strategy for fuel cell/battery/ultracapacitor hybrid vehicle considering fuel economy and fuel cell lifespan. *International Journal of Hydrogen Energy*, 45(15), 8875-8886. https://doi.org/10.1016/j.ijhydene.2020.01.017.
[9] JATO Dynamics Limited, 2020. www.jato.com.
[10] KASIMALLA, V.K.R., SRINIVASULU, G.N. & VELISALA, V., 2018. A review on energy allocation of fuel cell/battery/ultracapacitor for hybrid electric vehicles. *International Journal of Energy Research*, 42, 4263–4283. DOI: https://doi.org/10.1002/er.4166.
[11] MILLER, J.M., 2009. Energy storage system technology challenges facing strong hybrid, plug-in and battery electric vehicles. *Vehicular Power and Propulsion Conference 2009*. 4–10. DOI: https://doi.org/10.1109/VPPC.2009.5289879.
[12] MILLER, J.M., BOHN, T., DOUGHERTY, T.J., DESHPANDE, U., 2009. Why hybridization of energy storage is essential for future hybrid, plug-in and battery electric vehicles. 2009 *IEEE The Energy Conversion Congress and Exposition*. 2614–20. DOI: https://doi.org/10.1109/ECCE.2009.5316096.
[13] NEMRY, F., LEDUC, G., & MUÑOZ, A., 2009. Plug-in hybrid and battery-electric vehicles: State of the research and development and comparative analysis of energy and cost efficiency. *Joint Research Centre. Institute for Prospective Technological Studies*. Luxembourg. //ftp.jrc.es/pub/EURdoc/JRC54699_TN.pdf.

[14] OFFER, G.J., HOWEY, D., CONTESTABILE, M., CLAGUE, R., & BRANDON, N.P., 2010. Comparative analysis of battery electric, hydrogen fuel cell and hybrid vehicles in a future sustainable road transport system. *Energy Policy*. 38(1), 24–29. DOI: https://doi.org/10.1016/j.enpol.2009.08.040.

[15] PIELECHA, I., CIEŚLIK, W., & SZAŁEK, A., 2018. Operation of electric hybrid drive systems in varied driving conditions. *Eksploatacja i Niezawodnosc – Maintenance and Reliability*, 20(1), 16–23. DOI: https://doi.org/10.17531/ein.2018.1.3.

[16] PIELECHA, I., & PIELECHA, J., 2020. Simulation analysis of electric vehicles energy consumption in driving tests. *Eksploatacja i Niezawodnosc – Maintenance and Reliability*, 22(1), 130–137. DOI: https://doi.org/10.17531/ein.2020.1.15.

[17] POLAK, F., 2020. Energy balance comparison of small unmanned vehicle equipped with electric and hybrid propulsion system. *Combustion Engines*. 182(3), 23–27. DOI: https://doi.org/10.19206/CE-2020-304.

[18] POLSKIE STOWARZYSZENIE PALIW ALTERNATYWNYCH, 2020. www.pspa.com.pl.

[19] RAMBALDI, L., BOCCI, E., & ORECCHINI, F., 2011. Preliminary experimental evaluation of a four wheel motors, batteries plus ultracapacitors and series hybrid powertrain. *Applied Energy*, 88(2), 442–448. DOI: https://doi.org/10.1016/j.apenergy.2010.08.008.

[20] SHARMA, S., PANWAR, A.K., & TRIPATHI, M.M., 2020. Storage technologies for electric vehicles. *Journal of Traffic and Transportation Engineering*, 7(3), 340–361. DOI: https://doi.org/10.1016/j.jtte.2020.04.004.

[21] SUN, B., ZHANG, T., GE, W., TAN, C., & GAO, S., 2019. Driving energy management of front-and-rear-motor-drive electric vehicle based on hybrid radial basis function. *Archives of Transport*, 49(1), 47–58. DOI: https://doi.org/10.5604/01.3001.0013.2775.

[22] TAKAOKA, T., & ICHINOSE, H., 2010. The newly developed Toyota plug-in hybrid system. *31. Internationales Wiener Motorensymposium 2010*. Wien 2010.

[23] TIE, S.F., & TAN, C.W., 2013. A review of energy sources and energy management system in electric vehicles. *Renewable and Sustainable Energy Reviews*, 20, 82–102, DOI: https://doi.org/10.1016/j.rser.2012.11.077.

[24] VALDEZ-RESENDIZ, J.E., ROSAS-CARO, J.C., MAYO-MALDONADO, J.C., CLAUDIO-SANCHEZ, A., RUIZ-MARTINEZ, O., & SANCHEZ, V.M., 2020. Improvement of ultracapacitors-energy usage in fuel cell based hybrid electric vehicle. *International Journal of Hydrogen Energy*. 45(26), 13746–13756. DOI: https://doi.org/10.1016/j.ijhydene.2019.12.201.

[25] VUKAJLOVIĆ, N., MILIĆEVIĆ, D., DUMNIĆ, B., & POPADIĆ, B., 2020. Comparative analysis of the supercapacitor influence on lithium battery cycle life in electric vehicle energy storage. *Journal of Energy Storage*, 31, 101603. DOI:https://doi.org/10.1016/j.est.2020.101603.

[26] XIA, W., MAHMOOD, A., ZOU, R., & QIANG, X., 2015. Metal-organic frameworks and their derived nanostructures for electrochemical energy storage and conversion. *Energy & Environmental Science*, 8(7), 1837–1866. DOI: https://doi.org/10.1039/C5EE00762C.

[27] XIONG, R., DUAN, Y., CAO, J., & YU, Q., 2018. Battery and ultracapacitor in-the-loop approach to validate a real-time power management method for an all-climate electric vehicle. *Applied Energy*, 217, 153–165. DOI: https://doi.org/10.1016/j.apenergy.2018.02.128.

[28] YONG, J.Y., RAMACHANDARAMURTHY, V.K., TAN, K.M., & MITHULANANTHAN, N., 2015. A review on the state-of-the-art technologies of electric vehicle, its impacts and prospects. *Renewable and Sustainable Energy Reviews*, 49, 365–385. DOI: https://doi.org/10.1016/j.rser.2015.04.130.